PROC. OF JSCE
No. 292, December 1979

ULTIMATE STRENGTH OF STEEL ARCHES UNDER LATERAL LOADS

By Tatsuro SAKIMOTO and Sadao KOMATSU***

SYNOPSIS

The spatial elasto-plastic characteristics and the ultimate load carrying capacity of connected twin arches subjected to the combined loads of vertical and horizontal ones are studied. By using the numerical results for various numerical model arches, simple formula to design the lateral bracing member and to estimate the ultimate lateral strength of bridge arches are presented for a practical use.

1. INTRODUCTION

Ordinary bridge arches are composed of parallel twin ribs braced with lateral members to provide a sufficient lateral stability. There are now several investigations to show that the lateral bracing members play a very important role to increase the ultimate load carrying capacity of twin arches subjected to in-plane uniform loads[1)~6)]. It is needless to say that the bridge arches should be stable not only against the in-plane dead and traffic loads, but also against the lateral wind load and the lateral earthquake force[5)~10)]. The ultimate load carrying capacity of twin arches for these horizontal lateral loads is very important especially in Japan which is subjected to frequent attacks of a typhoon and a big earthquake. It is very possible that these horizontal lateral loads become governing design loads and they may cause a collapse of the bridge arch, because the bridge arch, which is an effective structural system for an in-plane uniform load, is not so favorable structural system for the lateral load. In this aspect, lateral bracing members are expected to have a direct contribution to the load carrying capacity of twin arches under the lateral load.

In a conventional design method, lateral bracing members and portal frames are intended to be dimensioned so as to be safe enough against the above-stated two kinds of lateral loads. But, the conventional design of the lateral bracing member is based on a simple beam theory and conducted independently of the design of the arch ribs. That is, the interaction between the arch ribs and the lateral bracing member is not considered at all. For example, the additional stress in the arch ribs due to these lateral loads is checked merely after the determination of all the cross-sectional dimensions. It may be reasonable, however, to design the arch ribs and the lateral bracing member under consideration of the spatial elasto-plastic large deflection behavior and the interaction between them.

The aim of this study is to clarify the spatial elasto-plastic characteristics and the ultimate load carrying capacity of twin arches subjected to the combined loads of vertical and horizontal ones in the above-stated aspects. By using the numerical results for various model arches, simple formula to design the lateral bracing member and to estimate the ultimate strength of bridge arches under the lateral load are presented.

2. NUMERICAL MODELS AND COMPUTATION METHOD

Numerical models named D 6 X and D 12 X, which have the spans of 100 m and 150 m, and 6 and 12 pairs of bracing members of double Warren type respectively, are considered as standard models for estimating the ultimate lateral strength of bridge arches. In order to maintain a possible generality of the obtained result for an application to actual bridge arches, the standard models are determined under consideration of the following items :

(1) The bridge arch treated is a two-hinged parabolic one that is composed of parallel twin ribs of prismatic box cross-section and connected each other with lateral bracing members of double Warren type in the central part of twin ribs. The bridge deck or the stiffening girder is not considered in the analysis.

* Dr. Engng., Assistant Professor of Applied Mechanics, Kumamoto University
** Dr. Engng., Professor of Civil Engineering, The Osaka University

(2) The rise-to-span ratio, f/l, of actual bridge arches falls between 0.1 and 0.2. Since its effect on the ultimate strength, which will be defined afterwards in a non-dimensional form, may be slight, the value of f/l is fixed to 0.1. The material is mild steel SS 41 of which the yield stress is 2 400 kg/cm^2 (=235 N/mm^2).

(3) Since the distance between both ribs, a, and the economical span, l, in ordinary solid-rib arches, seem to be from 5 m to 15 m and from 100 m to 150 m respectively, the distance a is fixed to the medium value, i.e., a=10 m and the span l is determined to be l=100 m and 150 m.

(4) As a through-type bridge is assumed, the twin ribs below the level of 4.5 m at least are not braced laterally for a traffic clearance requirement. For this requirement, the ratios, β, of the length of the braced portion to a total length of the arch rib are 0.59 for the model D 6 X and 0.79 for the model D 12 X. The direction of the in-plane uniform load is kept vertical during the lateral deformation of the arch rib, which means to neglect the stabilizing effect of the hanger load. This will give a conservative side value of the lateral strength for the actual hanger-loaded bridge arches.

(5) The height-to-width ratio h/b of the box cross section of arch ribs may vary from 1.0 to 3.0 in ordinary actual arches, but the ratio is limited herein to the medium value of h/b=2.0. The influence of the ratio h/b on the ultimate lateral strength of arches can be eliminated by using an adequate non-dimensional expression in the formula derived later.

(6) Referring to the several experimental results, a trapezoidal pattern of residual stress is assumed to be distributed on the cross section, where the maximum compressive residual stresses, σ_{rc}, are 40% of the yield stress, σ_y, for a mild steel and 20% for a high-strength steel SM 58. The maximum tensile residual stress is assumed to be equal to the yield stress.

(7) The panel length l_p of the double Warren truss is constant and equal to the rib distance a. The effective buckling length l_t of the bracing member is assumed to be $a/\sqrt{2}$. This value is obtained under the assumption of a hinged-hinged end condition of the member and the existence of the fictitious beams at the intersection points of the double Warren members.

(8) While the cross-sectional shape of the bracing member in ordinary arch bridges is angle, H or box, the box cross section having the same cross-sectional area as the hot-rolled H-shape is assumed for a simple treatment in the computer program. But, the mauimum axial force, N_t, which is computed as a minor-axis buckling load for a H-shaped section by using the standard strength curve for straight columns specified in the Japanese Specification for Highway Bridges[11], is used in the calculation to check a premature buckling of the truss member, which may occur prior to a collapse as a whole structure.

(9) A uniformly distributed vertical load, $\bar{p}$, is defined as the ratio of a design vertical load, p, to the uniformly distributed reference load, p_0, which produces the fully plastic normal force at the arch springings in the linear analysis. The vertical load, $\bar{p}$, which expresses the intensity of the dead and traffic loads, may vary from 0.2 to 0.6 in ordinary bridge arches.

One of the standard models is shown in Fig. 1 and other properties considered in the numerical model are summarized in Table 1. The slenderness ratio, λ_y, is defined herein as the ratio of the arc length of the arch rib, L, to the radius of gyration of the cross section, r_y, of the single rib with respect to lateral bending. The lateral load, q, is represented by the wind load, thereafter. In order to make a practical image of the strength, the ultimate strength, $\bar{q}$, under a lateral load is expressed here as the ratio of the ultimate lateral load, q_u, to a specified wind load, q_0. The reference wind load, q_0(kg/m), is estimated by the following equation :

$$q_0=\frac{1}{2}\rho V_w^2 C_d h \quad \cdots\cdots(1)$$

in which ρ=the density of air, 0.125 kg·sec/m^3, V_w =the wind velocity of 50 m/sec, C_d=the drag coefficient of arch rib, 2.19 for box cross section and h =the height of the arch rib in meter. Both the

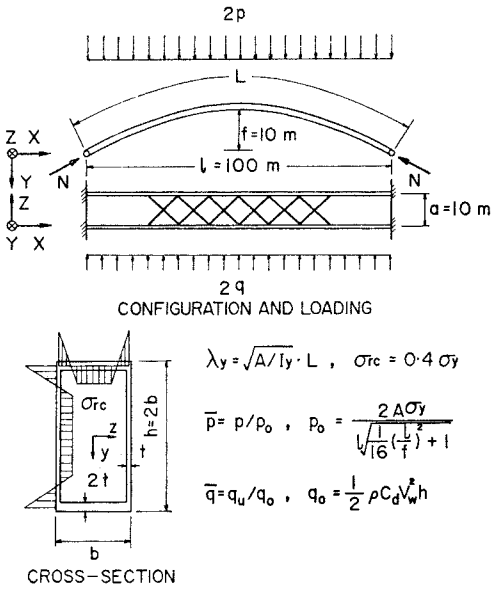

Fig. 1 Representative numerical model D 6 X.

Table 1 Basic Parameters of the Standard Models.

Items (1)	Properties (2)
configuration of arch	parabolic
span length l(m)	100, 150
rise-to-span ratio f/l	0.1
in-plane end conditions	hinged
shape of cross-section	welded box
section modulus ratio W_z/W_y	2.0
longitudinal variation of cross-section and material	uniform and homogeneous
distance of twin arches a(m)	10
lateral bracing system	double Warren
braced length ratio β	0.59, 0.79
slenderness ratio L/r_y	200, 300, 400
grade of steel E/σ_y	875
max. comp. residual stress	$0.4\sigma_y$
distribution of res. stress	trapezoidal pattern
initial lateral crookedness	none
in-plane load intensity $\bar{p}$	0.2, 0.4, 0.6
direction of in-plane load	vertical

windward rib and the leeward rib are supposed to be subjected to the identical wind load, q. In other words, so-called shielding effect is not considered. The value, $\bar{q}$, may be considered alternatively as a load factor for a design wind load of V_w=50 m/sec.

A general matrix stiffness method[12] developed for spatial large deflections and elasto-plastic behavior of thin-walled frames and arches with closed cross sections is used in evaluating the ultimate strength of the model arch. In numerical computations, each arch rib is divided into 14 and 16 member elements for the cases D 6 X and D 12 X, respectively. The truss member is treated as one member element, and the intersection point of double Warren truss is not treated as a nodal point because of the small effect on the result and for reducing the computational effort. The cross sections of the rib and of the bracing member are divided into 48 and 24 cross-sectional segments, respectively. The axial force of the truss member is kept constant after it attains the maximum value, N_t. This means that the truss member is considered to have no resistance against the additional force after the buckling. The lateral load, q, is increased under the constant in-plane load, p, step by step until the infinite increase in the lateral deflection due to an instability occurs. The ultimate lateral load, q_u, is defined herein by the average value of the last two loads which are the ultimate equilibrium load and the divergence in the next load step.

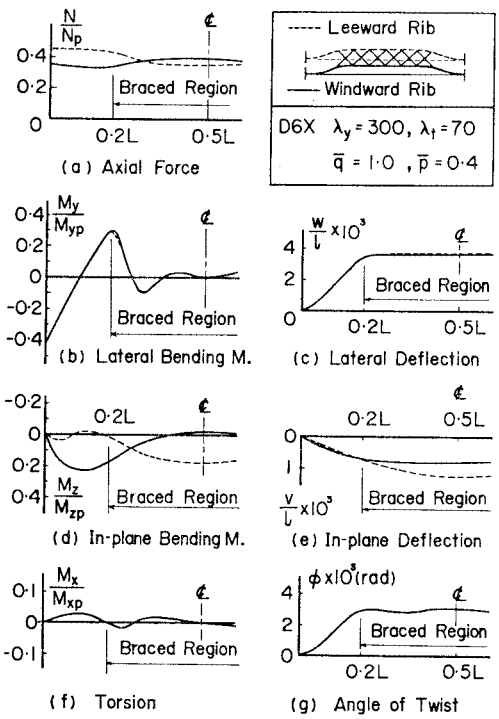

Fig. 2 Modes of stress resultants and deflections.

3. NUMERICAL RESULTS AND DISCUSSIONS

(1) Inelastic Spatial Characteristics of the Standard Models

Typical modes of the stress resultants and deflections are shown in Fig. 2, where N_p, M_{yp}, M_{zp}, and M_{xp} denote the full plastic values in axial force, bending moments about y, z-axes and torsional moment, respectively. These modes show, in general, similar characteristics to what observed in the ultimate state of the twin arches subjected to only the vertical load treated in the other paper[5]. The axial force of the windward rib is smaller than that of the leeward rib in the unbraced region, and vice versa in the braced region. This difference in the axial force between both rib may be caused by the cooperative lateral bending action of the both ribs against the lateral load.

The lateral bending moments of individual arch rib at the springings and the beginning parts of the braced region are large in relation to the large curvatures. The lateral bending moment in the braced region is fairly small except that in the edge panels, because the braced region is mainly displaced by a rigid body motion. The lateral bending moment decreases in the braced edge panel though it increases in the unbraced region. That is, the gradient of the moment diagram is negative in the braced edge panel. This negative gradient of the lateral bending moment diagram in the edge panel bears much importance in studying the axial force of the bracing members. The negative shear force due to this negative moment gradient induces an

additional axial force in the bracing member of the edge panel[10].

The shape of the in-plane bending moment diagram of the each rib is different from each other in relation to the respective in-plane deflection mode. The difference may be caused by the torsional action of the lateral horizontal force to the whole structure.

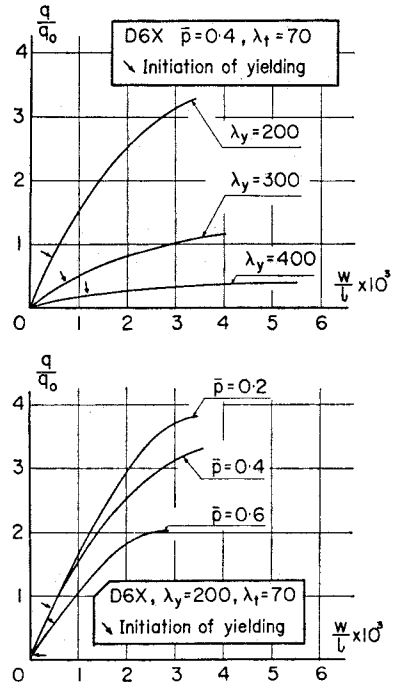

Fig. 3 Load versus lateral crown-deflection curves.

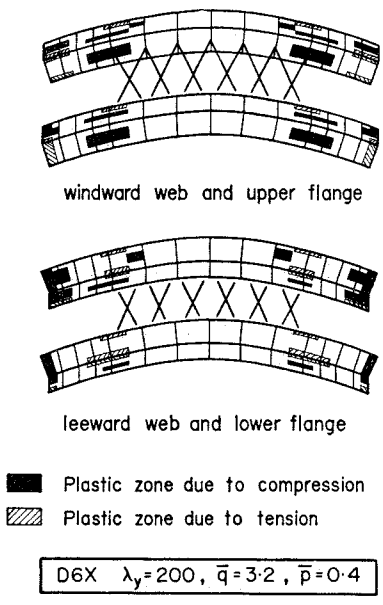

Fig. 4 Typical distribution of plastic zone at ultimate state.

Since the difference in the magnitude of the in-plane deflection between the both ribs can be intimately related to a torsional deformation of the integrated cross section composed of twin ribs, the difference in the in-plane bending moment between both ribs may correspond to the bi-moment for the integrated cross section. On the other hand, the torsional moment and the torsional angle of each rib are fairly small and their effects on the ultimate strength of twin arches may be negligibly small. All the characteristics stated above can be also seen in the numerical results of the case D 12 X.

Typical load versus lateral crown-deflection curves for the case D 6 X are shown in Fig. 3. The lateral bending stiffness, represented by the inclination of the curve, tends to decrease with an increase in the slenderness ratio, λ_y and the vertical load, $\bar{p}$. The large values of λ_y and $\bar{p}$ cause early yielding and also considerable reduction in the lateral bending stiffness, so that the lateral strength considerably decreases. The premature yielding initiates in the central part of web plates at the both springings. Typical distribution of the plastic zone is illustrated in Fig. 4. The plastic zones are restricted within the unbraced parts of ribs, and concentrated at the springings and both edges of the braced region. Tensile plastic zones also appear at the location where the convex curvature is produced by the lateral bending. The plastic zone of the leeward rib is a little larger than that of the windward rib, but there is not so appreciable difference between them.

(2) Ultimate Strength of the Standard Models

The lateral load carrying capacity of D 6 X is shown in Figs. 5 and 6. Fig. 5 shows the result for the twin arches with sufficiently rigid lateral bracings of slenderness ratio, $\lambda_t=70$. With the decrease in

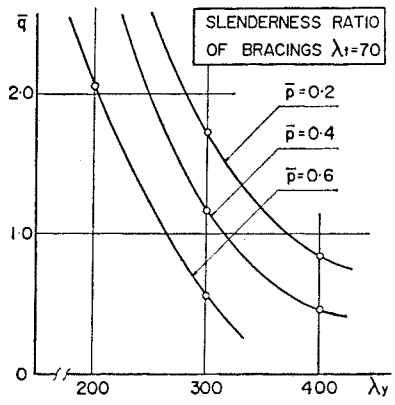

Fig. 5 Effect of in-plane load $\bar{p}$ on ultimate strength under lateral load (Model D 6 X).

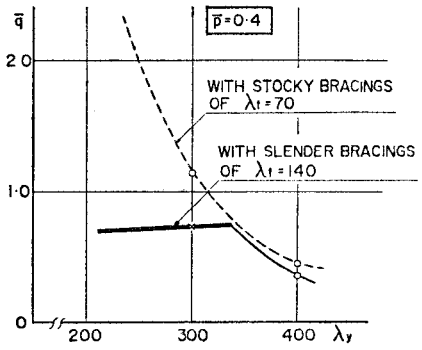

Fig. 6 Collapse due to premature buckling of lateral bracings (Model D 6 X).

specified values of both the vertical load, $\bar{p}$, and the slenderness ratio of arch ribs, λ_y, as is expected, the ultimate strength of the twin arches increases. Fig. 6 illustrates apparently the difference of the ultimate strength between the twin arches having lateral bracings of different slenderness ratios. In a range of λ_y from 200 to 350, there is a very fair possibility that the ultimate strength of twin arches is controlled by the buckling of lateral bracings as shown by the bold line. The premature buckling of lateral bracings occurs in the compressive members of the both edge panels, where the lateral shear force to be sustained by the lateral bracing is maximum. In these arches without portal beams, the overall structure collapses in such a way that it cannot have any margin of strength after the buckling of the bracings in the edge panels. The same phenomenon can be observed in the case of D 12 X as shown in Fig. 7 despite the fairly stocky lateral bracing of $\lambda_t=70$.

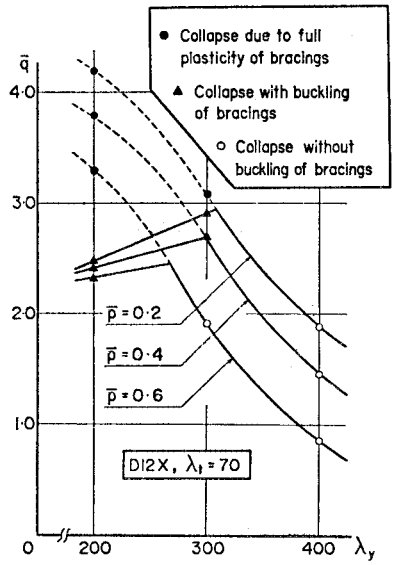

Fig. 7 Ultimate strength under lateral load (Model D 12 X).

The cause of the failure and the collapse mechanism are studied in elsewhere[10].

From these figures about the ultimate strength of the standard models D 6 X and D 12 X, the ultimate strength characteristics under the lateral load may be classified into three categories according to the slenderness ratio of the arch ribs, λ_y.

The stocky arch composed of members of closed cross section within the range of $\lambda_y<180$ may have enough ultimate strength as a single-rib arch under the lateral load. It might be said that there is no necessity of arranging the lateral bracing member so far as this analysis concerned. The twin arches of a medium slenderness ratio from 180 to 300 need the lateral bracing member for obtaining a sufficient ultimate strength. It is notable, however, that the ultimate strength of these arches will be controlled by the premature buckling of lateral bracings, therefore the lateral bracing and the portal frame should be carefully designed against the lateral load. A sufficient ultimate strength of the slender arch of $\lambda_y>300$ cannot be ensured even by much rigid lateral bracings, because it collapses owing to the reduction in lateral rigidity caused by the yielding in the rib near the springings. It is necessary to strengthen the ribs in the unbraced part and to prevent the premature yielding there.

(3) Relation between the Ultimate Strength and the Stress at the Springings

In order to confirm the fact that the ultimate strength of the slender arches of $\lambda_y>300$ under the lateral load may be controlled by the stresses at the arch springings, the ultimate strength of model arches named D 6 X·2 W_y is computed. For the case of D 6 X·2 W_y, the section modulus of ribs, W_y, within the unbraced parts is twice of that of the standard model. The ultimate strength of D 6 X·2 W_y under the lateral load is increased in the range of $\lambda_y>300$ as shown in Fig. 8. The models D 6 X·2 B and D 6 X·2 W_y·2 B are also treated for studying the effect of the rigid portal frame on the ultimate strength under the lateral load, where the moment of inertia of the portal beam, I_b, about the axis perpendicular to the arch rib is equal to that of the arch rib, I_y. The ultimate strength of D 6 X·2 B is remarkably increased in the range of $\lambda_y<300$ where the standard model D 6 X is controlled by the premature buckling of the slender bracing member as shown in Fig. 8. The ultimate strength of D 6 X·2 W_y·2 B under the lateral load is remarkably increased in all the range of slenderness ratio.

These facts show that there exists a close relation between the ultimate strength of twin arches and the stress at the springings. Then, the relation

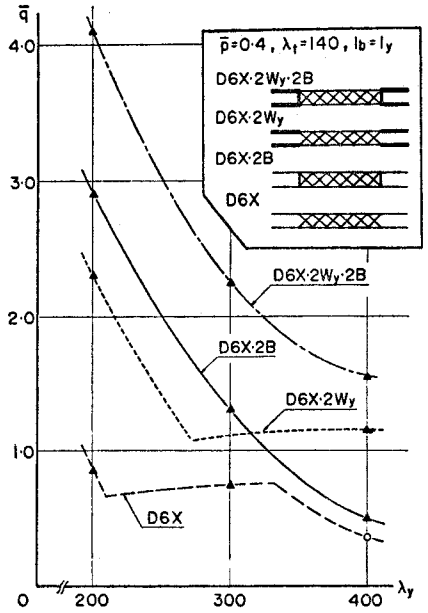

Fig. 8 Effects of the doubled section modulus and the portal beams.

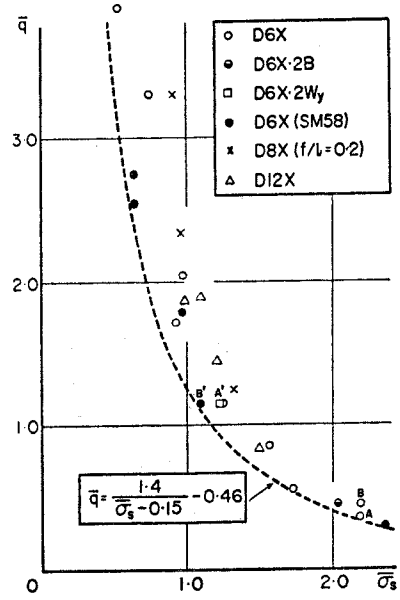

Fig. 9 Ultimate strength $\bar{q}$ versus representative stress at arch springings $\bar{\sigma}_s$.

between the ultimate strength, $\bar{q}$, and the maximum fiber stress, σ_s, at the springings of the leeward rib is studied for the model arches with the lateral bracing which never buckles. The non-dimensional stress $\bar{\sigma}_s$ is computed by

$$\bar{\sigma}_s=\frac{\sigma_s}{\sigma_y}=\frac{1}{\sigma_y}\left(\frac{N_s}{A_s}+\frac{M_s}{W_y}\right), \quad \cdots\cdots(2)$$

in which N_s=the normal force of the leeward rib computed by the elastic spatial analysis for the load stage $q/q_0=1.0$, A_s=the cross-sectional area of the rib at the springings, M_s=the lateral bending moment of the individual rib computed by the elastic spatial analysis for the load state $q/q_0=1.0$, W_y= the section modulus about y-axis of the individual rib, and σ_y=the yield stress of the material used in the arch springings.

Since $\bar{\sigma}_s$ can be regarded as a fictitious representative stress for the ideal elastic arch, the stress resultants N_s and M_s are obtained multiplying q_0/q by their values estimated at some load q lower than the elastic limit for the model arch which will collapse under the smaller load than q_0. Fig. 9 shows the relation between $\bar{q}$ and $\bar{\sigma}_s$, for various numerical models, where letters beside the plots denote the model name cited in the following. It may be confirmed by this figure that the ultimate strength of these twin arches under the lateral load may be a function of the stress $\bar{\sigma}_s$. Especially, this relationship can be understood very clearly from the following two facts. The ultimate strength of the model A'(D 6 X·2 W_y), which is related to the standard model A(D 6 X) is increased from 0.36 to 1.15 by decreasing the stress $\bar{\sigma}_s$ from 2.19 to 1.23. This is the result followed from doubling the section modulus of the individual rib in the unbraced parts. The ultimate strength of the model B'(D 6 X·SM 58) which is related to the standard model B(D 6 X) is also increased from 0.45 to 1.15 by using the high-strength steel called SM 58(σ_y=451 N/mm²). An approximate formula expressing a conservative relation between $\bar{q}$ and $\bar{\sigma}_s$ may be given by

$$\bar{q}=\frac{1.4}{\bar{\sigma}_s-0.15}-0.46. \quad \cdots\cdots(3)$$

Then, the ultimate strength of twin arches under the lateral load may be estimated by Eqs. 2 and 3. The method for predicting the stress σ_s by using simple frame model is studied in the next.

4. PRACTICAL FORMULAE

(1) Plane Frame Analysis of a Straightened Arch

Let us consider a laterally-loaded plane frame which is obtained by straightening the twin arches in the horizontal plane as shown in Fig. 10. Since this frame is an indeterminate structure of high order, it may be cumbersome to solve it analytically except by a matrix computer analysis. But, it can be solved approximately by noting the lateral bending characteristics shown in Fig. 2. That is, noting the fact that the lateral bending moment of the individual rib in the braced region abruptly decreases along the span length, the comparatively small bend-

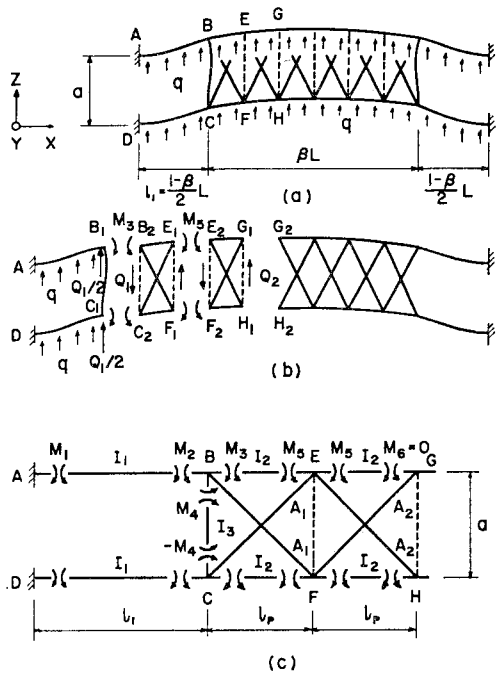

Fig. 10 Plane frame analysis for lateral bending moments of arch ribs.

ing moment in the central part may be disregarded. After all, the lateral bending moments of individual rib can be determined approximately by solving the sub-system which consists of a portal frame and two end panels.

Using the compatibility conditions upon the slopes at the points B and E, the unknown moments M_3 and M_5 can be determined and the frame can be easily solved. The slope of the point B_2, for example, may be approximated by the sum of the slope due to shear deformation of the panel and the slope of the arch rib as a simple beam subjected to end moments M_3 and M_5.

After some calculations, the lateral bending moments of the individual rib can be obtained as follows :

$$\left.\begin{aligned} M_1 &= -\frac{3k_3+1}{12k_3+2}Q_1l_1-\frac{4k_3+1}{12k_3+2}ql_1^2 \\ &\quad +\frac{1}{6k_3+1}M_3 \\ M_5 &= -\frac{1}{4}M_3+\frac{3}{4\sin\alpha\cos^2\alpha}\left(\frac{Q_1}{A_1}-\frac{Q_2}{A_2}\right)\frac{I_2}{l_p} \\ M_3 &= \frac{2k_2(3Q_1l_1+2ql_1^2)}{7+24k_2+42k_3} \\ &\quad -\frac{3(6k_3+1)\left(\dfrac{5Q_1}{A_1}-\dfrac{Q_2}{A_2}\right)\dfrac{I_2}{l_p}}{(7+24k_2+42k_3)\sin\alpha\cos^2\alpha} \end{aligned}\right\} \quad \cdots\cdots(4)$$

in which

$$k_1=\frac{I_1l_1}{I_1l_1}=1,\quad k_2=\frac{I_2l_2}{I_1l_p},\quad k_3=\frac{I_3l_1}{I_1a},$$

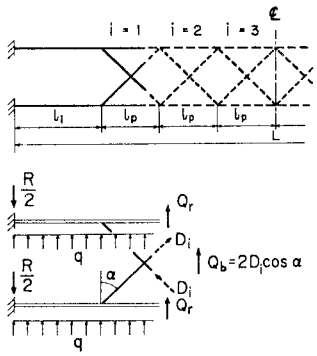

Fig. 11 Lateral shear resistance of twin arches.

$$l_1=\frac{1-\beta}{2}L,\quad Q_1=q\beta L,\quad Q_2=Q_1-2ql_p.$$

(2) Axial Force of Lateral Bracing Members

Noting Fig. 11, the axial force of the bracing member D_i in the i-th panel is given by

$$D_i=\left(\frac{1}{2}Q_i-Q_r\right)\sec\alpha, \quad \cdots\cdots(5)$$

in which Q_i=the shear force of the i-th panel, Q_r =the shear force of the individual rib and α=the angle between the bracing member and the normal of the arch rib. The shear force of the i-th panel, Q_i, is well approximated by the value of a simple beam theory as

$$Q_i=2\left[\frac{L}{2}-l_1-(i-1)l_p\right]q. \quad \cdots\cdots(6)$$

The shear force of the individual rib, Q_r, may be estimated as the derivative of the bending moment and approximated as follows :

$$Q_r=\frac{dM}{dx}\simeq-\frac{M_d}{l_p}, \quad \cdots\cdots(7)$$

in which M_d denotes the total variation of the lateral bending moment through the i-th panel as shown in Fig. 12 and is positive for a negative moment gradient. The value M_d in the edge panel ($i=1$) can be calculated by using the result of the prescribed plane frame analysis as

$$M_d=m(M_3-M_5), \quad \cdots\cdots(8)$$

in which the value m is amplification factor for so-called p-δ effect due to the interaction between the axial force of the arch rib and the lateral deflection. Considering the unbraced part of the arch rib as a column, the value m is defined by

$$m=\frac{N_E}{N_E-N}, \quad \cdots\cdots(9)$$

in which N=the axial force of the arch rib at springings and

$$N_E=\frac{\pi^2EI_1}{l_1^2},\quad l_1=\frac{1-\beta}{2}L. \quad \cdots\cdots(10)$$

The value M_d in the central panel, i.e., $i>1$, may be considered to be negligibly small and approxi-

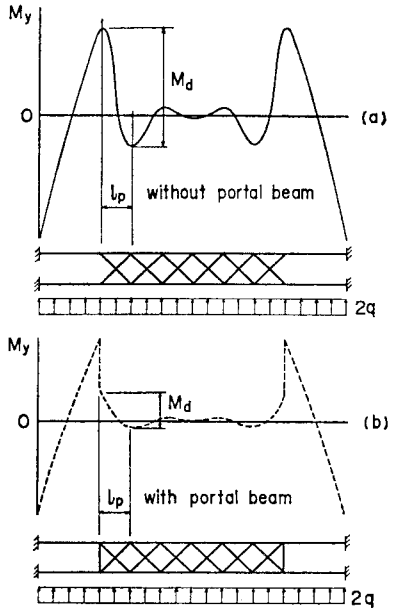

Fig. 12 Negative moment gradient in the edge panel.

mated to be $M_d=0$. Substituting Eqs. 6 through 10 into Eq. 5 gives the well approximated axial force of the bracing member.

It must be noted that Eqs. 5 through 10 include an iterative relationship, because the axial force from which the cross-sectional area of the bracing member should be determined cannot be computed without assuming the cross-sectional area. The lateral bracing members can be designed, however, by applying the standard column strength curve, after determining the axial force D_i by means of some trial and error method using together Eqs. 5 through 10.

Since the validity of the concept on which Eqs. 5 through 10 are based may not be affected by the type of lateral bracing systems, the equations may be applicable to other type of trussed bracings, for example, K-truss etc., after some modifications if necessary.

In a conventional design method, the shear force of the rib, Q_r, is neglected according to the assumption that all the shear force in the panel should be sustained only by the lateral bracing member. Hence, the axial force of the bracing member in a conventional design is given by

$$D_i=\frac{1}{2}Q_i \sec\alpha. \quad \cdots\cdots(11)$$

A representative relationship between the lateral load and the axial force of the bracing member in the edge panel is shown in Fig. 13. Fig. 13 shows that the conventional design method underestimates the axial force of the lateral bracing and gives an unfavorable value on the dangerous side. Therefore, it is seen that the shear force of the ribs may not be neglected especially for the twin arches with portal frames of insufficient stiffness. The proposed formula can predict the accurate value appropriately.

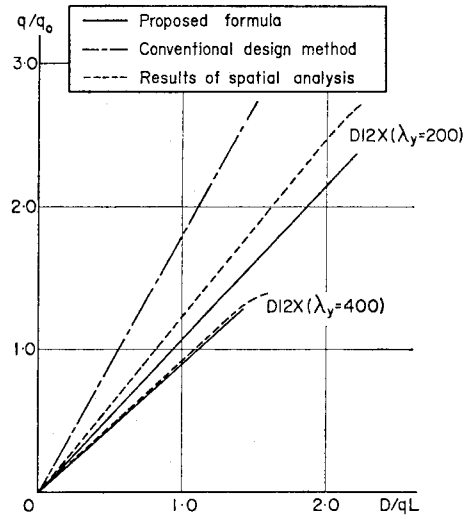

Fig. 13 Axial force of lateral bracing members in the edge panel.

(3) Estimation of the Maximum Stress at the Arch Springings

As stated previously, the ultimate strength of twin arches under lateral loads can be predicted by Eq. 2 which is a simple function of the maximum stress at the arch springings. The maximum stress at the arch springings σ_s can be estimated approximately without a cumbersome computer analysis by the sum of the three stresses σ_n, σ_i and σ_b shown in Fig.

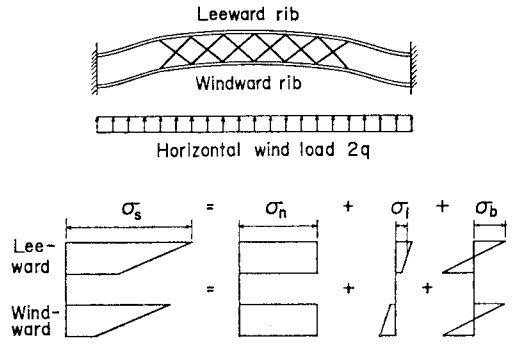

Fig. 14 Decomposition of stresses at arch springings.

14. That is,

$$\sigma_s=\sigma_n \quad \sigma_i+\sigma_b, \cdots\cdots(12)$$

in which σ_s=the maximum stress at the arch springings, positive for a compressive stress, σ_n=the average normal stress due to in-plane vertical uniform load, σ_i=the lateral bending stress calculated for an integrated system of twin ribs, and σ_b=the lateral bending stress for an individual bending of each rib. Each stress can be approximated by the following equations.

The average axial stress σ_n due to in-plane vertical uniform load is obtained by

$$\sigma_n=\frac{N}{A_s}, \cdots\cdots(13)$$

in which N=the normal force of arches at the springings in a linear theory. The value σ_i may be estimated by using the bending moment M_c[13] of circular curved-beam with both clamped ends shown in Fig. 15. The circular curved-beam is supposed to have an integrated cross section of twin arch ribs. In the case of a parabolic arch, a substitutive circular curved-beam whose configuration is determined from the three points of the both springings and the crown may be used. The equation is

$$\sigma_i=\frac{M_c}{A_s a}\beta, \cdots\cdots(14)$$

in which β=the ratio of the length of braced portion to the total length of arch, used as a reduction factor. At last, the value σ_b may be estimated by using the bending moment M_b computed by the plane frame analysis as follows :

$$\sigma_b=\frac{M_b}{W_y}m, \cdots\cdots(15)$$

in which M_b=the bending moment of the individual rib at the springings calculated for the plane frame $=-M_1$, W_y=the section modulus of the individual rib at the arch springings, and m=the amplification factor defined in Eq. 9. The estimated values of σ_s by Eqs. 13 to 15, σ_{se}, are compared with the values computed by the inelastic spatial analysis, σ_{sa}, for various numerical models in Fig. 16. Both values show good correspondence, and so σ_{se} can be used in Eq. 3 in place of σ_s.

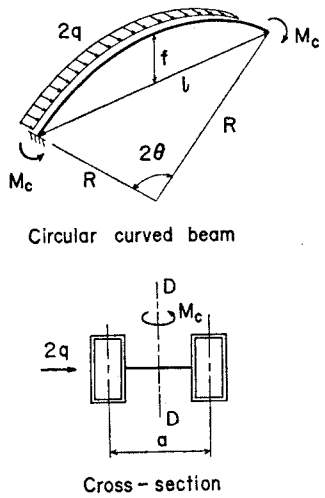

Fig. 15 Estimation of the bending stress σ_i as a circular curved beam.

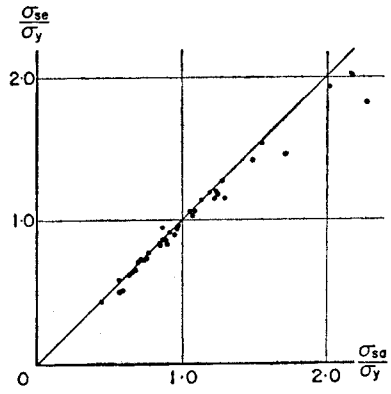

Fig. 16 Accuracy of the representative stress estimated by the proposed formula.

(4) Formulae for the Ultimate Strength

The ultimate strength of steel arches subjected to combined vertical and horizontal uniform loads may be given by the following formula :

$$\bar{q}=\frac{1.4}{\bar{\sigma}_s-0.15}-0.46, \cdots\cdots(16)$$

in which

$\bar{q}=q_u/q_0$, q_u=the ultimate lateral uniform load, q_0=the reference lateral load, for example, a design wind force,

$\bar{\sigma}_s=\sigma_s/\sigma_y$,

$$\sigma_s=\sigma_n+\sigma_i+\sigma_b=\frac{N}{A_s}+\frac{M_c}{A_s a}\beta+\frac{M_b}{W_y}m,$$

$$N=\frac{1}{2}\sqrt{\frac{1}{16}\left(\frac{l}{f}\right)^2+1}\,pl$$

: for parabolic arches,

$$N=\frac{3\theta(1+\sin^2\theta+2\sin^2\theta\cos^2\theta)}{6(\theta-3\sin\theta\cos\theta+2\theta\cos^2\theta)-\sin\theta\cos\theta(3+11\sin^2\theta)}pR$$

: for circular arches,

$$M_c=\frac{-(1-\theta\cot\theta)j+\dfrac{\theta}{\sin\theta\cos\theta}-1}{1+\dfrac{\theta}{\sin\theta\cos\theta}-j}2q_0R^2,$$

$$j=\frac{2E(Aa^2/4+I_y)}{GI_x+E(Aa^2/4+I_y)},$$

$$R=\frac{f}{2}+\frac{l^2}{8f},$$

$$M_b=\frac{3k_3+1}{12k_3+2}Q_1l_1+\frac{4k_3+1}{12k_3+3}q_0l_1^2-\frac{1}{6k_3+1}M_3,$$

$$M_3=\frac{2k_2(3Q_1l_1+2q_0l_1^2)}{7+24k_2+42k_3}-\frac{3(6k_3+1)}{(7+24k_2+42k_3)\sin\alpha\cos^2\alpha}\cdot\left(\frac{5Q_1}{A_1}-\frac{Q_2}{A_2}\right)\frac{I_2}{l_p},$$

$$k_2=\frac{I_2l_1}{I_1l_p},\quad k_3=\frac{I_3l_1}{I_1a},\quad l_1=\frac{1-\beta}{2}L,\quad Q_1=q_0\beta L,$$

$$Q_2=Q_1-2q_0l_p,\quad m=\frac{N_E}{N_E-N},\quad N_E=\frac{\pi^2EI_y}{l_1^2}. \qquad \cdots\cdots(17)$$

θ=the half of central angle of the arch,

A_s=the cross-sectional area of the individual rib at the arch springings,

I_x, I_y=the torsion constant and the moment of inertia about y-axis of the individual rib, use an average value weighted by partial length for variable cross sections,

A_1, A_2=the cross-sectional area of the bracing members in the edge and the next panels, respectively,

I_1, I_2=the moment of inertia of cross section of the individual rib in the portal range and in the edge panel, respectively, and

I_3=the moment of inertia of cross section of the portal beams=I_b.

The ultimate strength $\bar{q}_e$ estimated by the proposed formula is compared with the value $\bar{q}_a$ computed by the elasto-plastic spatial analysis for various numerical models in Fig. 17. The proposed formula gives fairly conservative predictions for the most of numerical models treated herein.

On using this formula it must be checked that the stress σ_n included in the stress σ_s is smaller than the value σ_u at which the arch fails owing to a lateral instability without the lateral load q. The ultimate stress σ_u of the arch subjected to only the in-plane uniform load can be obtained from the practical formula presented in the next section.

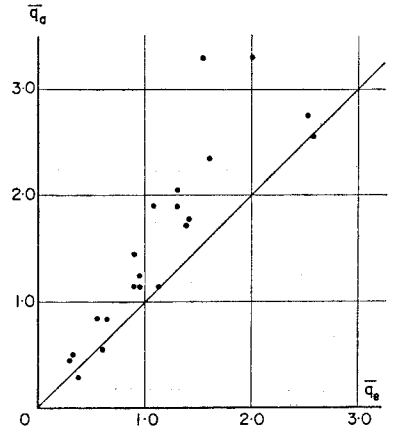

Fig. 17 Applicability of the proposed formula Eq. 16.

(5) Interaction Formula for the Ultimate Strength

The twin arches subjected to combined vertical and lateral loads may be intuitively considered to be analogeous to a beam-column. Accordingly, a Perry-Robertson type of formula may be also applicable to describe the ultimate strength of twin arches.

By the way, the ultimate stress, σ_u, of steel arches subjected to only the in-plane uniform load may be given in an identical equation to the standard column strength formula[11] by using an effective slenderness parameter, $\bar{\lambda}_y$. Detailed description for derivation of this formula is available in Ref. 6, and only the final result is given herein :

$$\left.\begin{aligned}&\bar{\sigma}=1-0.136\bar{\lambda}_y-0.300\bar{\lambda}_y^2 \quad \text{for } \bar{\lambda}_y\leqq 1.0\\&\bar{\sigma}=1.276-0.888\bar{\lambda}_y+0.176\bar{\lambda}_y^2 \quad \text{for } 1.0\leqq\bar{\lambda}_y\leqq 2.52\\&\bar{\sigma}=1/\bar{\lambda}_y^2 \quad \text{for } 2.52\leqq\bar{\lambda}_y\end{aligned}\right\}\cdots\cdots(18)$$

in which

$$\bar{\sigma}=\sigma_u/\sigma_y=N_u/A\sigma_y,$$

$$\bar{\lambda}_y=\frac{1}{\pi}\sqrt{\frac{\sigma_y}{E}}\frac{KL}{r_y},\quad r_y=\sqrt{\frac{I_y}{A}},$$

$$K=K_eK_\beta K_l,\quad K_\beta=1-(1-C)\beta,\quad C=2r_y/K_ea,$$

$$K_e=\begin{cases}0.5 & \text{for fixed end about lateral bending}\\1.0 & \text{for hinged end about lateral bending}\end{cases}$$

$$K_l=\begin{cases}0.65 & \text{for hanger-loaded arches}\\1.0 & \text{for vertically-loaded arches}\end{cases}$$

A=the cross sectional area of the individual rib, use an average value weighted by partial lengthes for a variable cross section, that is, $A=\sum_i A_iL_i/L$, $L=\sum_i L_i$,

σ_y=the yield stress, use the lowest value for hybrid arches,

N_u=the normal force at the arch springings in the ultimate state=$A\sigma_u$.

After all, the interaction formula for the ultimate strength of steel arches subjected to combined vertical and horizontal load may be given as follows :

$$\frac{N}{N_u}+\frac{N_E}{N_E-N}\frac{M}{M_y}=1.0 \qquad \cdots\cdots(19)$$

or

$$\frac{\sigma_n}{\sigma_u}+\frac{\sigma_b}{\sigma_y}=1.0 \qquad \cdots\cdots(20)$$

in which N=the normal force of arches defined in Eq. 17, N_E=the Euler buckling load for the arch rib of unbraced part, see Eq. 10, M=the lateral bending moment of the individual rib at the arch springings calculated for the plane frame=$-M_1$, see Eq. 3, and M_y=the yield moment of arch rib at the springings, σ_y=the yield stress of the material used at the arch springings.

The values (σ_n/σ_u, σ_b/σ_y) for the numerical models at the ultimate state are plotted in Fig. 18 together

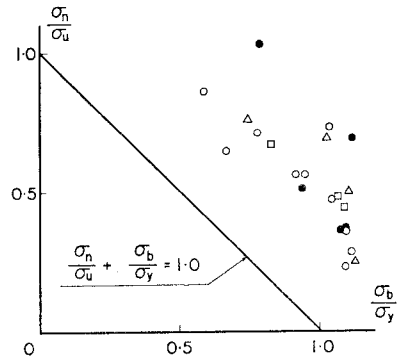

Fig. 18 Applicability of the interaction formula.

with the proposed formula. The numerical models of which bracing members buckled before reaching the ultimate state are omitted in the figure. Taking the possibility of local buckling of the component plates of the arch rib into account, this formula seems to be adequately conservative.

This type of formula is advantageous, because the load factors for the vertical load p and for the horizontal load q can be separated as will be performed in the design of beam-columns. Namely, denoting the load factors for the vertical load and the horizontal load by ν_p and ν_q, respectively, the design formula can be written as

$$\frac{\nu_p N}{N_u}+\frac{N_E}{N_E-\nu_p N}\frac{\nu_q M}{M_y}\leqq 1.0, \quad \cdots\cdots (21)$$

or

$$\frac{\nu_p \sigma_n}{\sigma_u}+\frac{\nu_q \sigma_b}{\sigma_y}\leqq 1.0. \quad \cdots\cdots (22)$$

5. SUMMARY AND CONCLUSIONS

In this paper, practical formulae for the ultimate strength of steel arches have been presented on the basis of the numerical results obtained for model arches. Though the numerical models are limited, these proposed formulae may be the basis for the future code studies. The results of this study can be summarized as follows :

(1) Modes of stress resultants and deflection show, in general, similar characteristics to what observed in the ultimate state of the twin arches subjected to only the vertical load treated in the previous paper.

(2) The lateral bending moments at the springings and the beginning parts of the braced region are considerably large in relation to the large curvature of the arch ribs due to lateral bending.

(3) The torsional moment and the torsional angle of each rib is fairly small and their effects on the ultimate strength of twin arches with closed cross sections may be negligibly small.

(4) The difference in the in-plane deflection and that in the in-plane bending moment between both ribs may correspond to the torsional angle and the bi-moment for the integrated cross section, respectively.

(5) The plastic zone due to lateral bending is remarkably developed in the ultimate state, but restricted to the springings and the beginning parts of the braced region.

(6) The ultimate strength characteristics of twin arches under the lateral load may be classified into three categories according to the slenderness ratio of the arch rib, λ_y, associated with the lateral bending.

(7) The twin arches with medium slenderness ratios from 180 to 300 need the lateral bracing member to provide a sufficient ultimate strength under the lateral load. But, the ultimate strength of these arches under the lateral load may have a possibility of being controlled by the premature buckling of lateral bracings, therefore a careful design of the lateral bracing and the portal frame is necessary.

(8) The sufficient ultimate strength of the slender arches with $\lambda_y > 300$ cannot be provided even by enough rigid lateral bracing systems, because they collapse owing to remarkable decrease in lateral rigidity caused by the yielding occurred in the ribs near the springings. In order to increase the ultimate strength, it is necessary to strengthen the arch ribs in the unbraced part and to delay the premature yielding there.

(9) It is notable that the shear force to be sustained by the bracing member becomes more than twice as much as the shear force predicted by a conventional design method based on a simple beam theory. This fact is caused by the negative shear force produced in the arch ribs. The axial force of the bracing member can be predicted more accurately by considering the total magnitude of the lateral bending moment variation through the edge panel.

(10) The lateral bending moment of the arch rib and the axial force of lateral bracing members of twin arches can be approximately calculated by analyzing a laterally-loaded plane frame which is obtained by straightening the twin arches in a horizontal plane. Using the results of the plane frame analysis, simple and approximate formula for estimating the axial force of lateral bracing members is proposed.

(11) The ultimate strength of twin arches under the lateral load is in close relation with the representative stress at the springings. A conservatively approximated formula expressing their relation is given in a simple form.

(12) The maximum stress at the arch springings can be simply and accurately approximated by the summation of three stresses found by using idealized plane frames. Then, the lowest value of the ulti-

mate strength of steel arches subjected to constant vertical load and horizontal uniform one may be given by a simple function of the maximum stress at the arch springings. The proposed formula can predict the lowest value of the ultimate strength of various numerical models very well, and may be applicable to the most of practical arches.

(13) An interaction formula for the ultimate strength of steel arches subjected to combined vertical and lateral load is also given taking advantage of the analogy between laterally-loaded arches and beam-columns. The proposed interaction formula can predict conservatively the ultimate strength of various numerical models. Since this type of formula is familiar to structural engineers, this formula will be convenient for a practical design purpose.

ACKNOWLEDGMENTS

The senior author wishes to acknowledge the eager encouragement that he received from Professor Dr. Itio Hirai of Kumamoto University. Numerical Computations were carried out by the digital computer FACOM 230-75 of the Computer Center, Kyushu University.

REFERENCES

1) Östlund, L. : Lateral stability of bridge arches braced with transverse bars, Transactions of the Royal Institute of Technology, Stockholm, Sweden, No. 84, 1954.
2) Kuranishi, S. : The torsional buckling strength of solid rib arch bridge, Transactions of JSCE, Vol. 75, pp. 59-67, July, 1961 (in Japanese).
3) Sakimoto, T. and Y. Namita : Out-of-plane buckling of solid rib arches braced with transverse bars, Proceedings of JSCE, No. 191, pp. 109-116, July, 1971.
4) Tokarz, F.J. : Experimental study of lateral buckling of arches, Journal of ST. Div., Proc. of ASCE, Vol. 97, No. ST 2, pp. 545-559, Feb., 1971.
5) Sakimoto, T., T. Yamao and S. Komatsu : Experimental study on the ultimate strength of steel arches, Proceedings of JSCE, Vol. 286, pp. 139~149, June, 1979.
6) Sakimoto, T. : Elasto-plastic finite displacement analysis of three dimensional structures and its application to design of steel arch bridges, Dissertation presented at Osaka University, Feb., 1979.
7) Kuranishi, S. and T. Yabuki : In-plane strength of arch bridges subjected to vertical and lateral loads, Preliminary Report of 2nd Int. Colloq. on Stability of Steel Structures, held at Liege, pp. 551-556, April, 1977.
8) Kuranishi, S. : Analysis of arch bridge under certain lateral forces, Transactions of JSCE, No. 73, pp. 1-6, March, 1961 (in Japanese).
9) Yabuki, T. and S. Kuranishi : Out-of-plane behavior of circular arches under side loadings, Proceedings of JSCE, No. 214, pp. 71-82, June, 1973.
10) Sakimoto, T. and S. Komatsu : A possibility of total breakdown of bridge arches due to buckling of the lateral bracings, Final Report of the 2nd Int. Colloq. on Stability of Steel Structures, held at Liege, Belgium in April, pp. 299-301, 1977.
11) Japan Road Association : Specifications for Highway Bridges, 1973.
12) Komatsu, S. and T. Sakimoto : Nonlinear analysis of spatial frames consisting of members with closed cross section, Proceedings of JSCE, No. 252, pp. 143-159, Aug., 1976.
13) Okamoto, S. : A study on circular curved beams subjected to lateral loads, Journal of JSCE, Vol. 20, No. 3, pp. 241-277, March, 1943 (in Japanese).

(Recieved December 26, 1978)